

Magnesium Removal from Aluminum Molten Alloy Using Enriched Mineral Zeolite with Amorphous Nano particles Of SiO_2

P. D. Pérez-Coronado, R. Muñoz-Arroyo, F. Garcia-Vazquez, H. M. Hdz-García, J.C. Escobedo-Bocardo, R. C. Tavitas-López, J. Acevedo-Dávila. COMIMSA-Salttillo, Ciencia y Tecnología No. 790, Col. Saltillo 400, 25290 Saltillo, Coah., México CINVESTAV Unidad Saltillo, Av. Industria Metalúrgica 1062, Parque Industrial Saltillo-Ramos Arizpe, 25900 Ramos Arizpe, Coahuila, México.

Abstract: In order to improve the Mg removal from an A-380 molten alloy, mixtures of mineral zeolite and amorphous silica nanoparticles ($\text{SiO}_{2(\text{NP}_s)}$) were tested. Zeolite was enriched with 1, 2 and 3 wt% of amorphous $\text{SiO}_{2(\text{NP}_s)}$. Before Mg removing, samples of mineral zeolite were impregnated with $\text{SiO}_{2(\text{NP}_s)}$ by mixed for 30 min in ethanol and then dried at 110°C for 24 h. The enriched zeolite with nanoparticles was analyzed by scanning electron microscopy and transmission electron microscopy. The Mg removal was carried out injecting each mixture into the molten aluminum alloy at 750°C using argon as a carrier gas. The Mg content of the molten alloy was measured after different periods of injection time (each 10 min). It was found that the mineral zeolite with 3 % of $\text{SiO}_{2(\text{NP}_s)}$ is the most efficient mixture, removing Mg from an initial content of 2 wt% to a final content of 0.046 wt%, in 70 min of injection. Moreover, thermodynamic predictions were carried out in the FactSage software in order to establish chemical equations occurring in the system.

Keywords: Zeolite, Aluminum, Nanoparticles, Amorphous Silica

I. INTRODUCTION

Aluminum is widely used in the manufacture and development of new products due to their excellent physical and chemical properties, mainly low density and high corrosion resistance [1]. So, it can be used in automotive and aerospace components. For this reason, the manufacture of aluminum alloys is basically focused in the increasing of the mechanical properties which is a prerequisite for the components that are subject to high stress. In this case, the Al-Si alloy has as mainly alloying elements Fe, Sb, Zn, Mn and Mg [2]. It is noticeable that a high content of Mg promotes the growth of the undesirable AlFeSi [3], [4]. Therefore, in aluminum foundries a variety of methods to Mg removal are used. The most usual method to remove Mg is chlorination [5]. Reports in the literature [5], [6] indicate that it is an efficient method to remove Mg. Nevertheless, this requires a strict control of storage and handling of chlorine gas as well as systems of filtration of gases in order to reduce contaminants. Other authors [2] report the use of reactive powders such as AlF_3 , MgCl_2 , KMgCl_3 , NaAlF_4 in order to remove Mg. These powders can clean and degasify the molten alloy. Besides, the kinetics of Mg removal is very slow and the treatment requires very long times. On the other hand, the electrochemical process is

another method that is used in the Mg removal and it is considered as a green-process [7]. However, it is necessary to consider that the cost of electricity in some countries is very high. In this way, the aim of this work was the study of the Mg removal from a A-332 molten aluminum alloy by using mixtures of mineral zeolite and $\text{SiO}_{2(\text{NP}_s)}$ as Mg remover agents. The capacity of these Mg remover agents was evaluated by comparing their effect with that corresponding to the mineral zeolite.

II. EXPERIMENTAL PROCEDURE

A. Raw Materials

The mineral zeolite from Coahuila, México was classified obtaining powders with an average particle size smaller than 150 μm . The chemical composition of the mineral was determined by atomic absorption spectroscopy, inductively coupled plasma atomic emission spectroscopy. Amorphous $\text{SiO}_{2(\text{NP}_s)}$ (Aldrich, 99.99%) with size smaller than 10 nm were selected for this work. These nanoparticles of SiO_2 were characterized by TEM and EDX.

B. Impregnation and characterization of mineral zeolite with amorphous $\text{SiO}_{2(\text{NP}_s)}$

The impregnation of mineral zeolite with amorphous $\text{SiO}_{2(\text{NP}_s)}$ (see Table I) were reached mixing the selected amount of nanoparticles (1, 2 and 3 %) with mineral zeolite for 30 min in ethanol and drying the mixture in a furnace at 110 °C for 24h. Samples of the enriched mineral silica were analyzed by SEM.

Table I. Mixtures of mineral zeolite with $\text{SiO}_{2(\text{NP}_s)}$ for 6 kg of Al-Si alloy.

Samples	Zeolite (g)	$\text{SiO}_{2(\text{NPS})}$ (g)
Zeolite	687.50	0
Zeolite+1% $\text{SiO}_{2(\text{NPS})}$	683.65	7.70
Zeolite+2% $\text{SiO}_{2(\text{NPS})}$	679.80	15.40
Zeolite+3% $\text{SiO}_{2(\text{NPS})}$	675.95	23.10

C. Thermodynamic predictions

Using the Gibbs free energy minimization algorithm implemented in the Equilib module of the FactSage package was considered in order to obtain

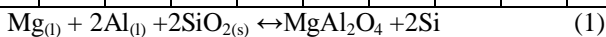
thermodynamics predictions using the stoichiometry (1) of the Section D and real experimental data. Likewise, in order to establish the reaction products as a function of increasing of SiO_{2(NP's)} impregnated in the mineral zeolite (1, 2 and 3%).

D. Experimental procedure for the Mg removal tests

The selected alloy was the A332 aluminum base alloy (Table II). An induction electric furnace, equipped with a silicon carbide crucible and temperature control, was used to melt and hold the alloy. Injection equipment, with devices to measure and control the gas and powder flows, was used to introduce the powder mixtures into the melt. The injection lance, with an internal diameter of 6.98 mm, was made of graphite. The selected parameters for the submerged powder injection experiments were argon (99.9999%) flow of 5 LAr/min, powder flow of 16g/min, mass of aluminum alloy of 6kg, and aluminum alloy treatment temperature of 750 °C. The lance was submerged at the 85% of the depth of the melt. The variable in the experiments was the composition of the powder mixtures zeolite-SiO_{2(NP's)} to be injected (0.0, 1, 2 and 3% of SiO_{2(NP's)}). The mass of the powders to be injected was calculated considering the SiO₂ as the solid reagent and spinel and silicon as products according to the chemical reaction (1).

Table II. Chemical composition (wt.%) of A332 aluminum alloy

Si (wt %)	Fe (wt %)	Mn (wt %)	Mg (wt %)	Cu (wt %)	Zn (wt %)	Ti (wt %)	Cr (wt %)	Ni (wt %)	Al (wt %)
11.64	0.849	0.026	2.000	0.410	0.040	0.128	0.010	0.032	Balance



For each experiment, samples of the melt were obtained every 10min and the produced dross (oxidized material) was collected at the end of the experiment. The solidified samples were analyzed by spark atomic emission spectrometry to determine their chemical compositions and a sample of the dross was analyzed by XRD. Additionally, the quantity of slag was weighted and the efficiency of process was calculated by using (2).

Efficiency:

$$\eta = \frac{\%Mg_i - \%Mg_f}{\%Mg_i} \quad (2)$$

Where: %Mg_i is the initial percent of magnesium and %Mg_f is the final percent of magnesium. Thermodynamic

predictions about the studied system were carried out using the FactSage software.

E. Characterization of Reaction Products

In order to determine the reaction products, samples of the slags formed during the injection tests were characterized by X-ray diffraction (XRD) brand PHILLIPS model X'PERT PW3040.

III. RESULTS AND DISCUSSIONS

A. Raw Materials Characterization

Table III shows the chemical composition, obtained by atomic absorption, of mineral zeolite. As can be seen, silica is 56.090 wt% and the H₂O that it can influence to removal Mg by oxidation. Reports in the literature [8], [9] suggest that silica can remove the Mg of molten alloys using the injection method of enriched-silica powders when the initial Mg content is 1.0wt% [9].

Table III. Chemical composition of mineral zeolite obtained by atomic absorption.

Mineral	K (wt %)	Ca (wt %)	Na (wt %)	Al (wt %)	SiO ₂ (wt %)	Fe (wt %)	Mg (wt %)	Sr (wt %)	H ₂ O (wt %)
Zeolite	1.410	1.430	0.058	6.080	56.090	1.510	0.400	<0.005	12.018

Fig. 1(a) shows the mineral zeolite as received. Fig. 1(b) presents a SEM image of particles of this material with plates shaped material (Carlsbad's twin) and the corresponding EDX which indicates that the particles are composed of zeolitic minerals.

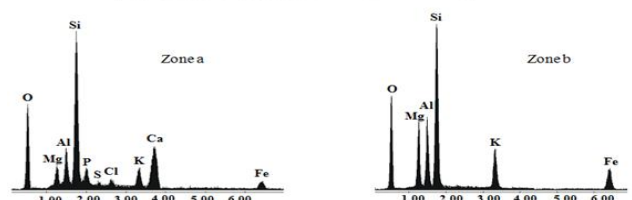
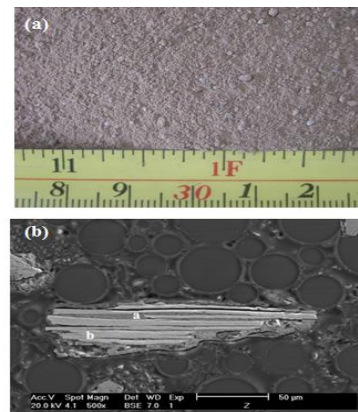


Fig. 1. Mineral zeolite: (a) as received and (b) SEM image (Carlsbad's twin) and EDX of mineral zeolite without nanoparticles of amorphous SiO₂(NP's).

of the reactions varying the content in g of SiO₂(NP's) at 750°C, 1 atm and considering 21 g of O₂ (Table IV).

B. Characterization of the enriched mineral zeolite with amorphous SiO₂ (NP's)

Amorphous SiO₂(NP's) nanoparticles as received and a sample of mineral zeolite with 3 % of SiO₂(NP's) were analyzed by TEM (Fig. 2 (a) and (b)). At high amplification, it is observed that the SiO₂(NP's) have a spherical morphology as received (Fig. 2(a)). The enriched mineral zeolite with 3 wt% of SiO₂(NP's) shows nanoparticles agglomerates at different zones (Fig.2(b)). This surface aspect can affect the rate and time of Mg removal due to that increase the surface energy by the nanoparticle sizes, increasing the reaction kinetics.

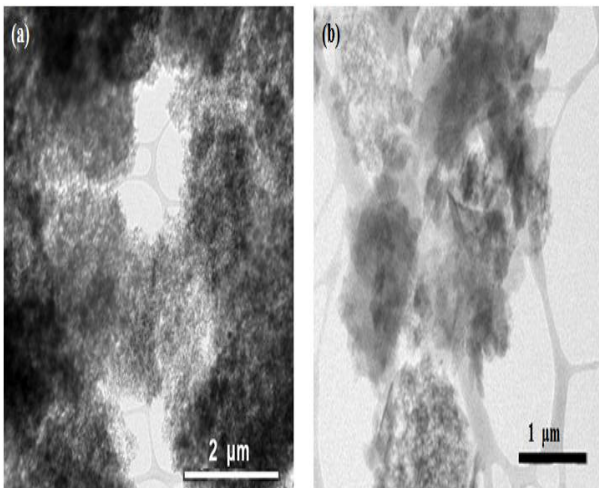


Fig. 2. TEM images: (a) amorphous SiO₂ nanoparticles as received and (b) impregnated mineral zeolite with 3 % of SiO₂(NP's).

C. Thermodynamic predictions and selection of the Al Alloy and Mg removal by Injection

In regards to Eq. 1 and considering the KAlSi₃O₈ zeolitic compound with 3 % of SiO₂(NP's), the feasibility thermodynamic of this reaction was determined in the Equilib module of FactSage. Based in this equation and considering the amount of Mg in the alloy, calculations with 1 and 2 % of SiO₂(NP's) were performed. As can be seen in the Fig. 3, at least the formation of spinel and Si with 3% of SiO₂(NP's) are predicted by using (1), as proposed in literature [8].

Therefore, as a preliminary step to the removal process of Mg were carried on thermodynamic predictions simultaneously with real experimental data in the FactSage package as follows: 1) First, a series of calculations were made in the Equilib module in order to obtain the Gibbs free energy minimization and 2) in the Reaction module was illustrated the graph of free energy

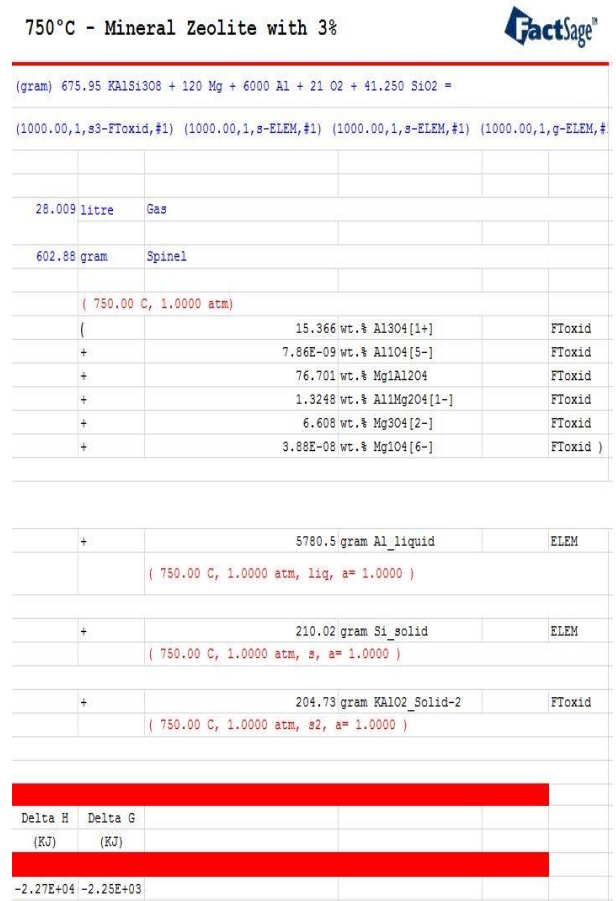


Fig.3. Thermodynamic predictions calculated in the Equilib module of FactSage.

Table IV. Amounts of reactants considered for Mg removal, calculated at 750 with 21 g of O₂ using the Equilib and Reaction modules of FactSage.

Reaction	Al-Si (kg)	Mg (kg)	SiO ₂ (NP's) (g)
Zeolite	6	0.120	0
Zeolite+1% SiO ₂ (NPS)	6	0.120	7.70
Zeolite+2% SiO ₂ (NPS)	6	0.120	15.40
Zeolite+3% SiO ₂ (NPS)	6	0.120	23.10

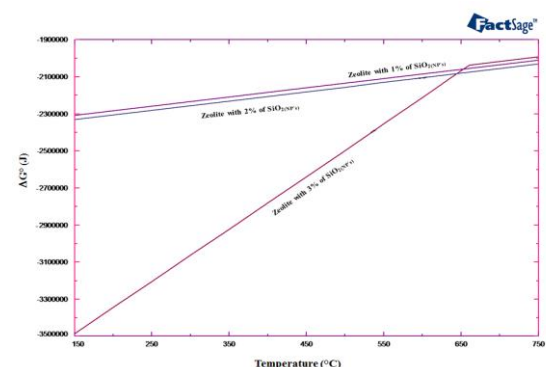


Fig.4. Diagram of Gibbs free energy for Mg removal calculated in FactSage.

As can be seen in the Fig. 4, the Gibbs free energies is more spontaneous when the content of 3 % of SiO_{2(NP s)}. But at 650°C the reaction increases the free energy slowing the reaction. This fact shows that the removal of Mg can be carry out faster than the other two reactions with 1 and 2 % of SiO_{2(NP s)}.

D. Experimental procedure for the Mg removal tests

Figure 5 shows the variation of the Mg content in the aluminum alloy as a function of the injection time for the different experiments at 750°C. As it can be observed in Fig.5, when mineral zeolite is used Mg is removed from its initial concentration (2 wt%) to a final concentration of 0.6 wt%. By contrast, the best results were obtained when a mixture containing 3 % of SiO_{2(NP s)} was used, reaching a final Mg concentration of 0.046 wt% for 70 min. This behavior can be explained considering that the increase of the surface energy due to the silica nanoparticles and the stirring conditions into the molten alloy created by the magnetic induction forces of the furnace and the carrier gas flow, contribute to the Mg removal. The amount of Mg removed from the molten alloy was a direct function of the amount of nanoparticles in the mixture mineral zeolite-SiO_{2(NP s)}. Comparatively, the Mg removal is faster the first 10 min with 3 % of SiO_{2(NP s)} and, this result is consistent with the predictions of free energy (Fig. 4).

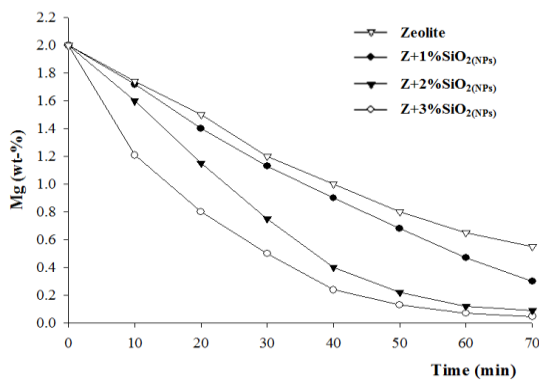


Fig.5 Mg content in the alloy as a function of the injection time for the performed experiments at 750°C.

Table V shows the Mg removal efficiency (η) for each experiment. It is noticeable that the efficiency increases in the mixtures of mineral zeolite with 2 and 3 wt% of SiO_{2(NP s)} due to the surface energy of the mineral silica is modified by the impregnated nanoparticles, this fact

increases the kinetics of Mg removal. On the other hand, it was further observed that by using mixtures of mineral silica and nanoparticles, a smaller amount of slag was generated. In addition, stable oxides such as MgAl₂O₄(spinel), MgO(periclase) and Mg₂SiO₄(forsterite) as well Ca_{5.16}Si₃₆O₇₂·(H₂O)_{21.8} (clinoptilolite) are formed and they were identified in the slag by XRD as can be seen in the Table VI.

Table V. Relationship feed weight (initial ingot) to the final weight (final ingot) and efficiency (η).

Muestra	W _{initialing} of (kg)	W _{finaling} of (kg)	W _{sla} g (kg)	%M g initial	%M g final	η (%)
Zeolite	6	3.90	1.240	2	0.600	70
Z+1%SiO _{2(NP s)}	6	2.62	0.863	2	0.300	85
Z+2%SiO _{2(NP s)}	6	2.71	0.549	2	0.090	95.5
Z+3%SiO _{2(NP s)}	6	3.58	0.498	2	0.046	97.7

Table VI. Main reaction products identified in the slag by XRD analysis.

Compound	Zeolite	Z+1%SiO _{2(NP s)}	Z+2%SiO _{2(NP s)}	Z+3%SiO _{2(NP s)}
Al	X	X	X	X
Si	X	X	X	X
SiO ₂ quartz	X	X	X	X
AlN	X			
MgO periclase	X	X	X	X
MgAl ₂ O ₄ spinel	X	X	X	X
Mg ₂ (SiO ₄) forsterite	X	X	X	X
Al ₂ O ₃ corundum	X			
Ca _{5.16} Si ₃₆ O ₇₂ ·(H ₂ O) _{21.8} Clinoptilolite	X			

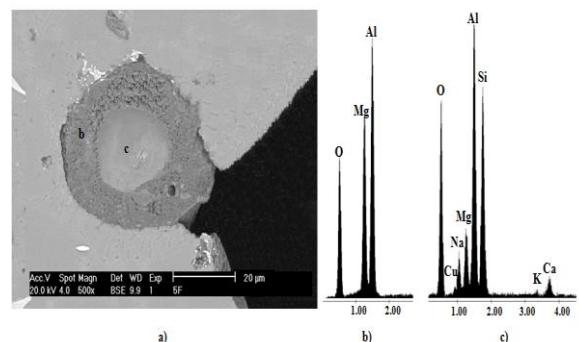


Fig.6.a) SEM image of a semi-reacted zeolite particle and corresponding EDX; b) shell of spinel and c) zeolite unreacted center.

It has been postulated that the decrease in the Mg removal rate is due to the formation of a spinel shell on the surface of the mineral zeolite particle, shell that continuously grows. According to the chemical reaction (1), spinel is a final product with high thermodynamic stability. A semi-reacted zeolite particle is observed in Fig. 6, showing a shell of spinel on the surface of an unreacted mineral zeolite nucleus.

IV. CONCLUSIONS

Mineral zeolite enriched with 3 % of $\text{SiO}_2(\text{NP}_s)$ demonstrated its capacity as Mg remover from 2 to 0.046 wt% for 70 min. The Mg removal rate from the molten alloy is reduced due to the formation of a spinel shell on the surface of the silica particles. It is noticeable that the use of this mineral zeolite with SiO_2 nanoparticles reduces the amount of generated slag, decreasing the metal losses by oxidation. In addition, it was found that the Gibbs free energy minimization algorithm for the Mg removal can be predicted through the combination of Equilib and Reaction modules in order to establish a balance of mass. This innovative technology using Nanotechnology can be applied to obtain aluminum ingots with high Mg contents in order to make automotive components. This work requires an economic evaluation of the process times to decrease the Mg in the A380 aluminum alloys. However, the enriched mineral zeolite with nanoparticles of silica can be applied to remove high content of Mg until 0.1 wt.% to obtain an A380 alloy that is established by the ASTM Handbook.

V. ACKNOWLEDGEMENT

The authors wish to express their gratitude to the National Council of Science and Technology (CONACyT) and COMIMSA for supporting the development of the postdoctoral fellow of Rita Muñoz Arroyo.

REFERENCES

- [1] Samuel, F. & Gowri, S., Effect of Mg on the Solidification Behavior of Two Al-Si-Cu-Fe-Mg (380) Diecasting Alloys. Transactions of the American, Vol. 101, pp.611-618, 1993.
- [2] Gaustad, G., Olivetti, E. & Kirchain, R., Improving aluminum recycling: A survey of sorting and impurity removal technologies. Resources, Conservation and Recycling, Vol. 58, pp. 79-87, 2012.
- [3] Gowri, S. & Samuel, F., Effect of Alloying Elements on the Solidification Characteristics and Microstructure of Al-Si-Cu-Mg-Fe 380 Alloy. Metallurgical and materials transactions, Vol. 25 A, pp. 437-448, 1994.
- [4] L. Anantha Narayanan, F. H. Samuel, J. E. Gruzleski, Crystallization Behavior of Iron-Containing Intermetallic

Compounds in 319 aluminum Alloy. Metallurgical and materials transactions, Vol. 25 A (8), pp.1761-1773, 1994.

- [5] E. A. Vieira, J.R. De Oliveira, G. F. Alves, D. C. R. Espinosa, J. A. S. Tenorio, Materials Transactions, Vol. 53 (3), pp. 477-482, 2012.
- [6] V. D. Neff V. y P. B. Cochran; Light Metals, U. S. A., Panel for Aluminum Processing, Vol. 1993, pp. 1053-1060, 1993.
- [7] B. L. Tiwari, B. J. Howie y R. M. Johnson, AFS Transactions, U. S. A., pp. 385-390, 1986.
- [8] R. Muñoz A., J. C. Escobedo B., H. M. Hdez-G., D. A. Cortés H., M. Terrones M., A. Rodríguez P., J. L. Hernández P.; Revista de Metalurgia, Vol. 46 (4), pp. 1988-4222, 2010.
- [9] F. Carmona-Muñoz, H. M. Hdz-García, R. Muñoz-Arroyo, J. C. Escobedo-Bocardo, D. A. Cortés-Hernández, Chemical Technology, An Indian Journal, Vol. 8 (4), pp. 115-120, 2013.